Asian Journal of Atmospheric Environment
Vol. 7-1, pp.25-37, March 2013
doi: http://dx.doi.org/10.5572/ajae.2013.7.1.025

Modeling of Emissions from Open Biomass Burning in Asia Using the BlueSky Framework

Ki-Chul Choi, Jung-Hun Woo*, Hyeon Kook Kim, Jieun Choi[1)], Jeong-Hee Eum[2)] and Bok H. Baek[3)]

Department of Advanced Technology Fusion, Konkuk University, Seoul, Korea
[1)]Department of Environmental Engineering, Konkuk University, Seoul, Korea
[2)]Department of Landscape Architecture, Keimyung University, Daegu, Korea
[3)]Institute for the Environment, The University of North Carolina, Chapel Hill, NC, USA

*Corresponding author. Tel: +82-2-2049-6022, E-mail: jwoo@konkuk.ac.kr

ABSTRACT

Open biomass burning (excluding biofuels) is an important contributor to air pollution in the Asian region. Estimation of emissions from fires, however, has been problematic, primarily because of uncertainty in the size and location of sources and in their temporal and spatial variability. Hence, more comprehensive tools to estimate wildfire emissions and that can characterize their temporal and spatial variability are needed. Furthermore, an emission processing system that can generate speciated, gridded, and temporally allocated emissions is needed to support air-quality modeling studies over Asia. For these reasons, a biomass-burning emissions modeling system based on satellite imagery was developed to better account for the spatial and temporal distributions of emissions. The BlueSky Framework, which was developed by the USDA Forest Service and US EPA, was used to develop the Asian biomass-burning emissions modeling system. The sub-models used for this study were the Fuel Characteristic Classification System (FCCS), CONSUME, and the Emissions Production Model (EPM). Our domain covers not only Asia but also Siberia and part of central Asia to assess the large boreal fires in the region. The MODIS fire products and vegetation map were used in this study. Using the developed modeling system, biomass-burning emissions were estimated during April and July 2008, and the results were compared with previous studies. Our results show good to fair agreement with those of GFEDv3 for most regions, ranging from 9.7 % in East Asia to 52% in Siberia. The SMOKE modeling system was combined with this system to generate three-dimensional model-ready emissions employing the fire-plume rise algorithm. This study suggests a practicable and maintainable methodology for supporting Asian air-quality modeling studies and to help understand the impact of air-pollutant emissions on Asian air quality.

Keywords: Open biomass burning, Atmospheric emissions, MODIS, BlueSky Framework, Asia

1. INTRODUCTION

Open biomass burning in Asia is an important contributor to air pollution in the region. Definitions used for "open biomass burning" in this study is defined as field biomass burning, such as man-made and/or natural forest fires and savanna/grassland burning. For certain pollutants, their emissions comprise approximately 20-30% of the Asian total emissions (Streets *et al.*, 2003). Exposure to open biomass burning (e.g., wildfire) smoke is associated with increased eye and respiratory symptoms, medication use, physician visits, and exacerbated asthma (Kuenzli *et al.*, 2006). Open biomass burning also affects the global climate through emissions of greenhouse gases and aerosols, and through the reduction of vegetation cover (Yevich and Logan, 2003).

From this viewpoint, it is important to accurately estimate emissions from open biomass burning using diverse data and methods. Streets *et al.* (2003) quantified the amount of "typical" (i.e., non-year-specific) emissions from open biomass burning based on published ground-based report data. Woo *et al.* (2003) estimated the contributions of biomass, biofuel, and fossil-fuel sources to the air masses observed during the TRACE-P experiment. Michel *et al.* (2005) developed an emissions inventory of Asian open biomass burning based on the GBA2000 algorithm. Globally, the Global Fire Emissions Database, Version 2 (GFEDv2), which was recently updated to GFEDv3, offers a gridded fire-emissions inventory covering the globe (van der Werf *et al.*, 2006). However, these studies were performed based on month-long aircraft field campaigns (Michel *et al.*, 2005; Woo *et al.*, 2003) or had relatively coarse spatiotemporal resolution (van der Werf

et al., 2006; Streets *et al*., 2003). Although the GFED inventory has been widely used among experts, it is aimed at global-scale studies, and it supports only 0.5° gridded data per month. Hence, it has limited fire characteristics for regional-scale studies, especially in terms of temporal and spatial resolution.

Thus, a more comprehensive framework is needed for estimating biomass-burning emissions over Asia. Accurate temporal and spatial estimates of biomass-burning emissions, however, are not easy to determine using conventional statistics because of the random nature of the fires. Moreover, burning estimates based on government or institute reports from Asian countries are quite limited.

The BlueSky Framework, developed by the US Forest Service (USFS) and the US Environmental Protection Agency (EPA), is a modeling framework designed to facilitate the operation of predictive models that simulate cumulative smoke impact, air quality, and emissions from forest, agricultural, and range fires. It is simply a model management framework that offers the architecture for multiple and varied models to communicate with each other in a modular, user-driven environment (Pryden, 2008). This framework can be combined with the SMOKE (Sparse Matrix Operator Kernel Emissions) system, which generates better spatiotemporal distributions of open-burning emissions and better representation of the vertical structures of burning plumes.

The aim of this research is to implement the BlueSky Framework for modeling Asian biomass-burning emissions to simulate the impact of open biomass burning on air quality. To accomplish this, biomass-burning emissions in Asian regions were estimated and a new Asian fuel map was developed. Finally, the BlueSky framework was combined with the SMOKE modeling system to improve the air-quality modeling. This study suggests a practicable and maintainable methodology to support Asian air-quality modeling studies and to help to understand the impact of air-pollutant emissions on Asian air quality.

2. METHODOLOGY

2.1 Overview of Implementation of the BlueSky Framework for Asia

The method used to calculate emissions was based on the BlueSky modeling framework. The BlueSky framework allows users to choose one of several models in each processing step. The models used in this study were FCCS (Fuel Characteristic Classification System) for the fuel loading process, and CONSUME and EPM (Emissions Production Model) for estimating fuel consumption and open-burning emissions, respectively. The BlueSky-EM (Emissions Model) derived from the BlueSky framework contains two modules (CONSUME and EPM) that together are used to estimate emissions based on the work of Sandberg and Peterson (1984). The CONSUME total fuel consumption model considers both flaming and smoldering components, and it is available for most forests, shrubs, and grasslands (Ottmar *et al*., 1993). The EPM model, which estimates emissions from wildland biomass burns, uses emission factors for each pollutant to estimate burning emissions on a per-fire basis. Emission estimates are calculated on the basis of two combustion stages, and then summed to estimate total emissions. Equation 1 shows the emission estimates equation applied to the flaming stage of a burning period (Sandberg and Peterson, 1984).

$$E_{F,t} = A \times W_f \times EF_F / TIGN \quad (1)$$
$$\text{When } TFLAM < t < TIGN$$

where $E_{F,t}$ is the flaming-stage emissions; A, burned area; W_F, flaming-stage fuel consumption; EF_F, emission factor for the flaming stage; TFLAM, start time for uniform flaming; and TIGN, ignition time.

Three mapped fuel loadings are available in this initial version of the BlueSky framework: the FCCS (Mckenzie *et al*., 2004; Sandberg *et al*., 2001), the Hardy (Hardy *et al*., 1998), and the National Fire Danger Rating System (NFDRS) (Burgan *et al*., 1998). As mentioned above, the FCCS fuel loadings were used in this study because they have a more detailed fuel classification scheme than others.

MODIS (Moderate Resolution Imaging Spectroradiometer) instruments on board the Terra and Aqua satellites provide the fire information (burned area product) for the fuel-loading estimates, as well as land cover data for biomass classification (Land cover type 1-IGBP, International Geosphere-Biosphere Programme). We used these satellite measurements to estimate biomass-burning emissions.

Although BlueSky is a powerful and flexible framework, it is strongly oriented to application in the United States. In order to build a successful emissions system for Asia, the processing of fire information and the development of a fuel map associated with a fuel classification based on regional characteristics, fire characteristics such as fire-plume rise, chemical compounds, as well as the modification of system codes are required. In addition to all of the Asian countries considered in the previous study of Streets *et al*. (2003), Siberia and Kazakhstan (40N-70N, 60E-180E) were also included in our biomass-burning emissions domain to incorporate the strong Siberian forest fires (Jeong *et al*., 2008; Lee *et al*., 2005; Tanimoto *et al*., 2000). Daily emissions from each fire event were used

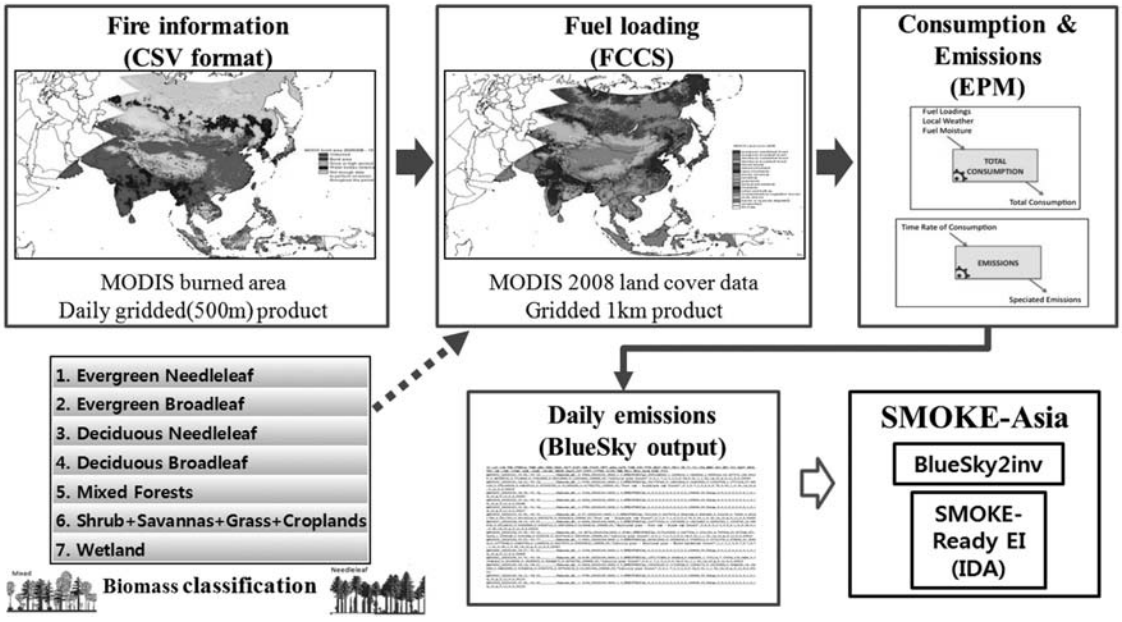

Fig. 1. Biomass-burning emissions modeling framework for Asia.

to create day-specific input files readable by SMOKE, which could be easily linked to the SMOKE modeling system. We estimated biomass-burning emissions during April and July 2008 for initial validation.

The overall framework for modeling biomass-burning emissions in Asia (here we refer to it as BlueSky-Asia) is shown in Fig. 1.

2.2 Fire Information

In this study, we used the MODIS Burned-Area Product (MCD45A1) (Roy *et al*., 2005) to estimate the emissions from open biomass burning in our domain for April and July 2008. The MODIS burned-area (BA) based fire information has a relatively high (i.e., daily) temporal resolution and medium (i.e., 500-m grid) spatial resolution. MODIS burned-area products use a bi-directional reflectance model based on a change detection algorithm to estimate the burned area with a resolution of 500 m (Roy *et al*., 2002). They are saved daily as polygons in a cumulative shape file, along with the associated latitude and longitude information for the fire polygon center, number of burned area pixels detected, date of detection of the burned area, and the name of the administrative region. The burned-area pixels are considered to be part of the same fire event when they are detected in the same day and area within a distance of one pixel (500 m). Each fire event is represented by one polygon containing the number of burned-area pixels detected (total area burned), date of burning, and geographical location, and this polygon is used as an input for the plume-rise calculation for each fire event, as well as for emissions from the biomass-burning calculation.

Other products available from MODIS are active fire or thermal anomalies (Aqua: MYD14A2, Terra: MOD 14A2). The MODIS active-fire (AF) product detects fires in 1-km pixels that are burning at the time of overpass under relatively cloud-free conditions using a contextual algorithm. The thresholds are first applied to the observed middle-infrared and thermal-infrared brightness temperature and then false detections are rejected by examining the brightness temperature relative to neighboring pixels (Giglio *et al*., 2003). The products were downloaded from the NASA anonymous FTP server (ftp://e4ftl01u.ecs.nasa.gov). A comparison between burned-area and active-fire products is useful to understand environmental spatiotemporal fire characteristics and remote-sensing factors. Furthermore, it can highlight the planning needs for the validation of the MODIS burned-area product (Roy *et al*., 2008). Hence, we discuss and analyze the MODIS fire products for our domain in detail in section 4.

2.3 Fuel Map

The fuel map is one of the most important pieces of information for the fuel-loading process to estimate biomass-burning emissions in the BlueSky Framework. Although the fuel map in the FCCS (Fuel Characteristic Classification System) is the most comprehensive one, it was developed to be used in the United States. For this reason, we have tried to develop a new fuel map for Asia using the MODIS 2008 land cover pro-

duct (MCD12Q1, Land cover type 1-IGBP). The MOD 12Q1 Land Cover Product supplies an IGBP (International Geosphere-Biosphere Programme) land cover classification map (Belward *et al*., 1999; Scepan, 1999) of the globe along with an assessment of the quality or confidence that is placed in that classification.

Thirteen vegetation classes used in the land cover map were reclassified to 7 classes to match the FCCS fuel beds (Table 1). The land cover map was then reprojected to the Lambert Azimuthal projection to create fuel beds with 1-km grid resolution and converted to a netCDF file, which is the FCCS import format (Fig. 2).

2.4 Linking the BlueSky Framework to the SMOKE Modeling System

The Sparse Matrix Operator Kernel Emission (SMOKE) is a processing system that creates model-ready emissions to support regional-scale atmospheric chemical models such as the Community Multiscale Air Quality (CMAQ) modeling system (Houyoux *et al*., 2007). As explained in Section 2.1, the BlueSky framework is a tool to predict the cumulative impact of emis-

Table 1. Reclassified vegetation class for fuel-loading process in BlueSky Framework.

IGBP vegetation class	Reclassified in this study
Evergreen needleleaf forest	Evergreen needleleaf forest
Evergreen broadleaf forest	Evergreen broadleaf forest
Deciduous needleleaf forest	Deciduous needleleaf forest
Deciduous broadleaf forest	Deciduous broadleaf forest
Mixed forests	Mixed forests
Closed shrublands	
Open shrublands	
Woody savannas	
Savannas	Shrub+Savannas+Grass+
Grasslands	Croplands
Croplands	
Cropland/natural vegetation mosaic	
Permanent wetlands	Wetland

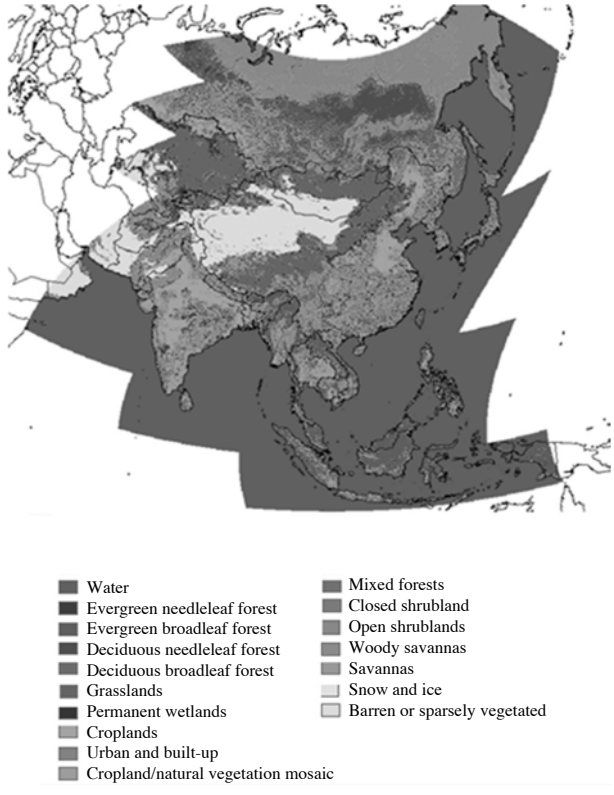

Fig. 2. Fuel loading map for FCCS in Asia (2008).

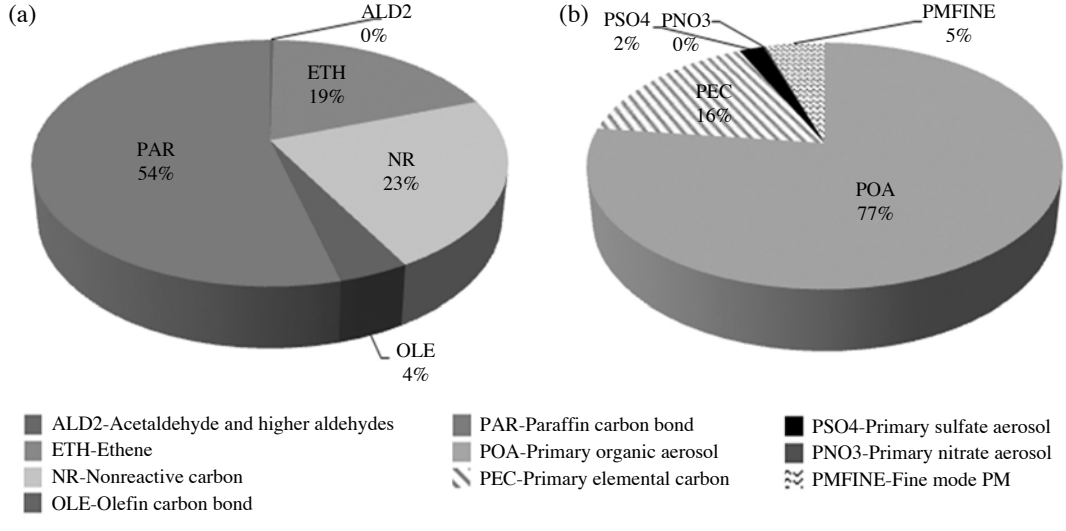

Fig. 3. Chemical speciation (% in mass) of (a) VOCs and (b) $PM_{2.5}$ for biomass-burning sources.

sions from forest, agricultural, and range fires. By combining these two tools, temporally and spatially accurate open biomass burnings can be modeled, and furthermore, simulation of the impact of emissions on air quality can be enhanced.

Biomass-burning emissions are treated as point sources rather than area sources. This allows the plume-rise scheme caused by the strong buoyancy of emitted hot gases to be considered and can provide an opportunity to examine the effect of plume rise on long-range transport. To calculate the plume rise from biomass-burning emissions more realistically, the heat flux output from BlueSky (equation 2) is used to generate a buoyancy flux using equation 3 (Anderson *et al*., 2004).

$$Q = CR_{Tot} \times C_{Eff} \times B_{Eff} \times E_{Eff} \times h \times 2000 \quad (2)$$

where CR_{Tot}=Total consumption rate (ton/h)
C_{Eff}=Combustion efficiency
B_{Eff}=Buoyant efficiency
E_{Eff}=Entrainment efficiency
h=Heat of combustion (BTU/lb)
2000=Pounds per ton

$$F = Q \times 0.00000258 \quad (3)$$

where F=buoyancy flux (M^4/s^3)
Q=heat flux (BTU/h)

Plume rise for open biomass burnings is calculated using the Briggs plume-rise algorithm. In SMOKE version 2.2 or higher, the ability to model the plume rise of wildfires was added. Detailed processes to integrate the two models (the BlueSky and the SMOKE)

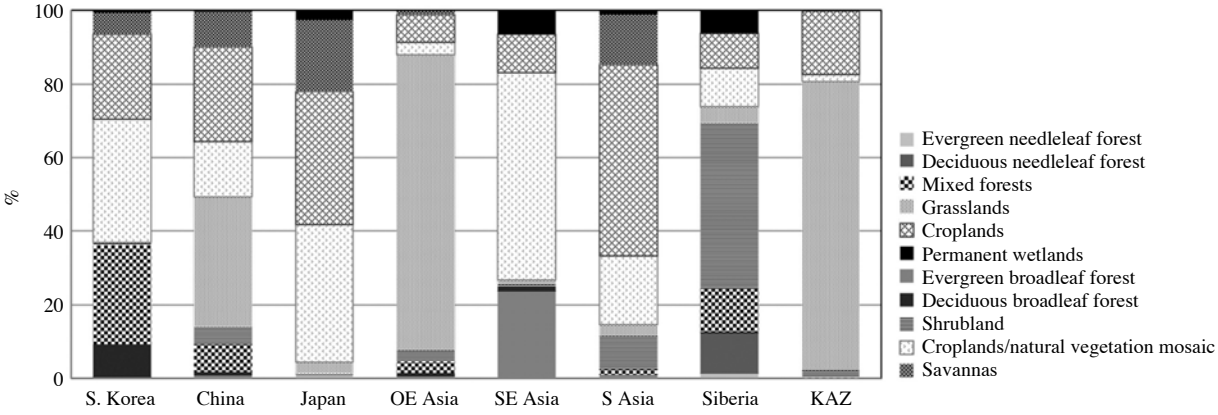

Fig. 4. Portion of total vegetated area for each region (KOREA: South Korea; OEASIA: Mongolia, North Korea, Taiwan; SEASIA: Southeast Asia; SASIA: South Asia; KAZ: Kazakhstan).

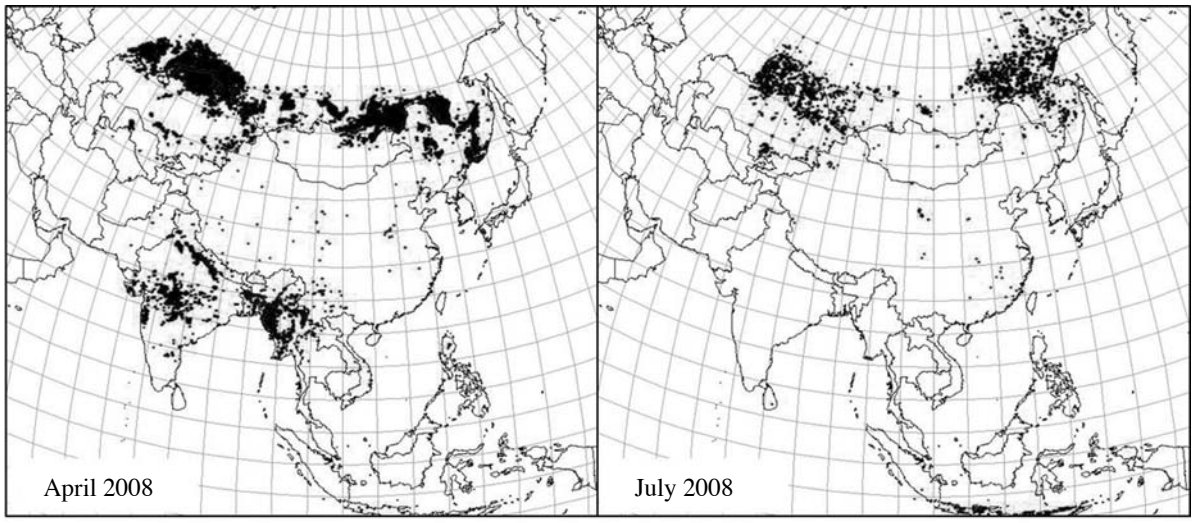

Fig. 5. Detected burned area pixels based on MODIS burned-area products.

were implemented based on the work of Pouliot *et al.* (2005).

The SMOKE system is also capable of converting "inventory species" into "model species" through its chemical speciation process for different chemical mechanisms (Houyoux *et al.*, 2007). In our study, a lumped structure mechanism, the Carbon Bond Mechanism Version IV (CB4), was adopted. Chemical profiles for VOCs and $PM_{2.5}$ were applied to the biomass-burning sources. A selection of VOCs and $PM_{2.5}$ species are shown in Fig. 3. The major constituents of the VOCs and $PM_{2.5}$ were paraffin and organic aerosols, mostly due to the emissions from open biomass burning of forest, savanna, or grassland, and from the burning of crop residues in fields.

3. RESULTS FROM BLUESKY-ASIA DEVELOPMENT

3.1 Development of the Fuel Map and Total Burned-area Information

We used the MODIS land cover product (MCD12Q1, Land cover type 1-IGBP) to define the vegetation classes in our domain. Fig. 4 shows the portion of vegetation types for each region based on the MODIS 2008 land cover product. The main vegetation types are grasslands and croplands, which represent approximately 24% and 23% of the total vegetation area, respectively.

Fig. 5 shows the burned-area pixels detected in our domain during April and July 2008. The total number of burned acres was calculated by region using the MODIS burned-area products (MCD45A1). The regions included were China, South Korea, Japan, OEASIA (Other East Asia, including N. Korea, Mongolia, Taiwan), SEASIA (South East Asia), SASIA (South Asia),

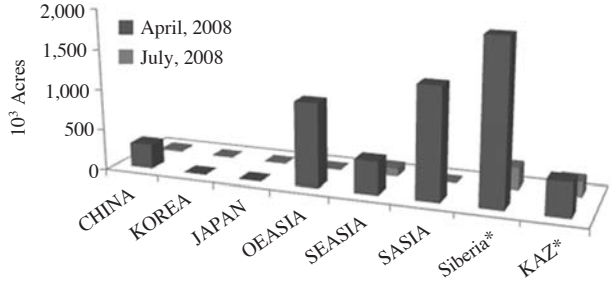

Fig. 6. Total burned area for each region (KOREA: South Korea; OEASIA: Mongolia, North Korea, Taiwan; SEASIA: Southeast Asia; SASIA: South Asia; KAZ: Kazakhstan; *burned area for Siberia & KAZ are multiplied by 10^{-1}).

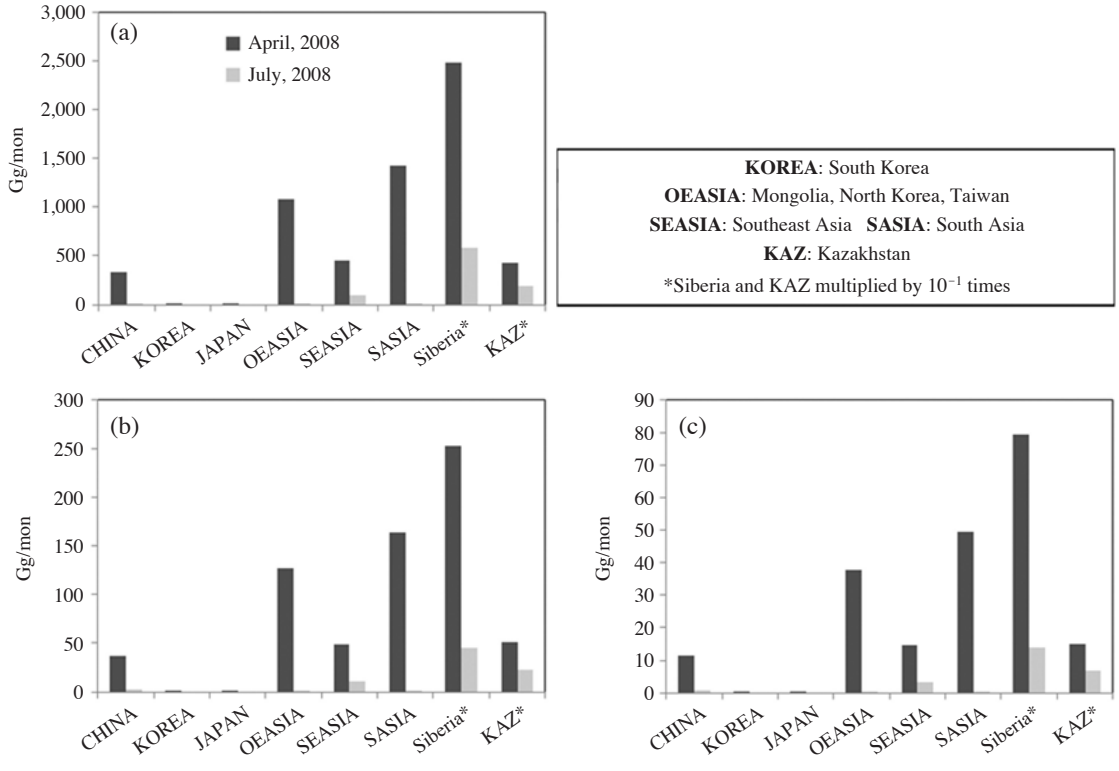

Fig. 7. Emission estimates of biomass burning for each region in our modeling domain: (a) CO, (b) $PM_{2.5}$, (c) NMHC.

Siberia, and KAZ (Kazakhstan) (Fig. 6). For April, the burned areas were approximately five times larger than those for July, which was mainly caused by Siberian fires. It is also shown, that the burned areas of Kazakhstan in April were three times larger than those in July. Overall, the regions included in our domain had much greater burned areas in April than July, mainly because of interference from monsoon cloud formation and rainfall in July.

3.2 Biomass-burning Emission Estimates

In this study, biomass-burning emissions were estimated using the BlueSky Framework for Asia during April and July 2008. Even though we have mainly presented CO emissions, other pollutants like $PM_{2.5}$ and NMHC (non-methane hydrocarbons) were also estimated. Fig. 7 presents the estimated biomass-burning emissions for each region in our domain. The biomass-burning emissions show a similar spatiotemporal distribution to the burned areas, which is one of the most important factors for estimating biomass-burning emissions. High CO emissions were found in OEASIA and SASIA during April, but these regions showed lower CO emissions during July. This is because the Asian monsoon caused smaller burned areas and the cloud interferences caused less detection in July and thus resulted in lower CO emissions. Relatively, Siberia had higher CO emissions than other regions during the target period. $PM_{2.5}$ and NHMC also show similar spatiotemporal distributions for CO emissions.

3.3 Initial Air-quality Modeling Using Developed Model-ready Emissions

As explained in Section 2.4, emission estimates from the BlueSky Framework can be easily combined with the SMOKE modeling system to allow better temporal and spatial representation of biomass-burning emissions. We created model-ready emissions using the SMOKE modeling system with the BlueSky Framework for the period April 03-16 and July 14-27 to support regional-scale chemical-transport modeling. The modeling periods were selected for regional urban-scale chemical-transport modeling using CMAQ (MOE, 2009). A series of daily fire emission inventories were created using the BlueSky framework and the emissions were further processing the SMOKE modeling

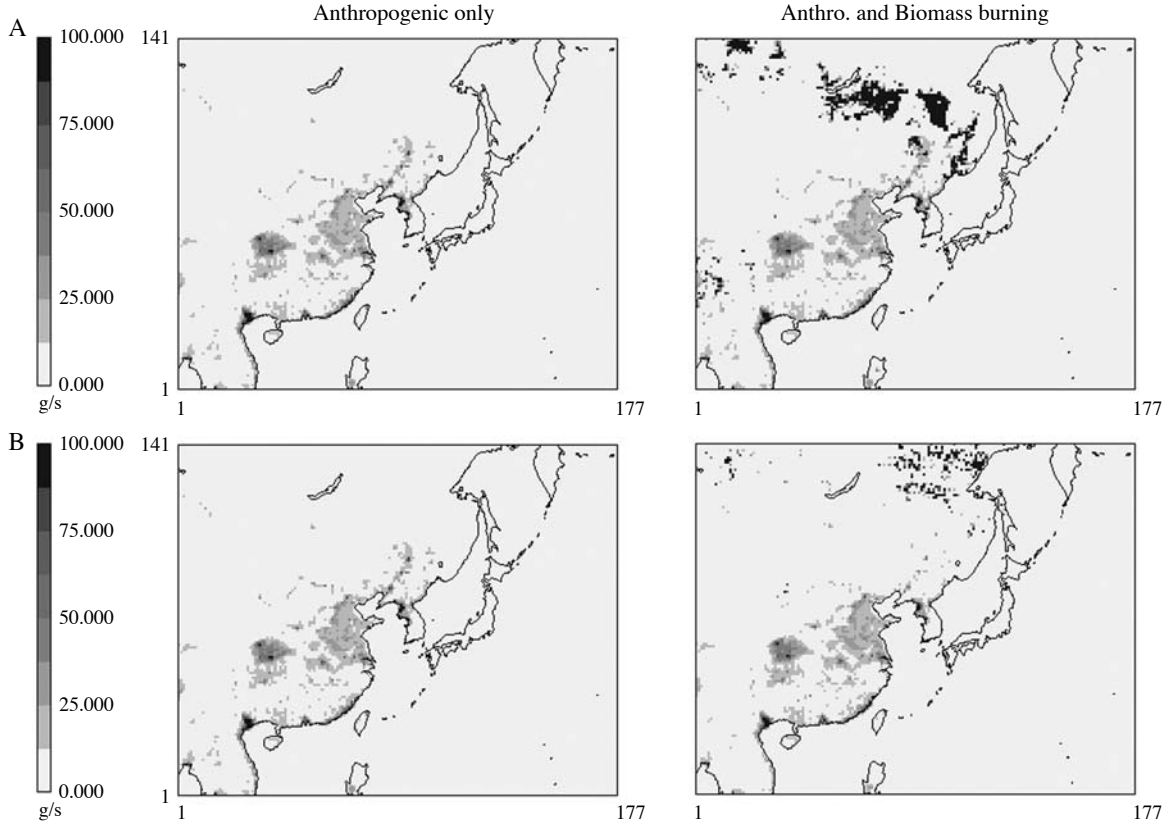

Fig. 8. POA gridded emission from anthropogenic sources and integrated sources of anthropogenic and biomass-burning sources during the modeling period (A: 03-16 April; B: 14-27 July).

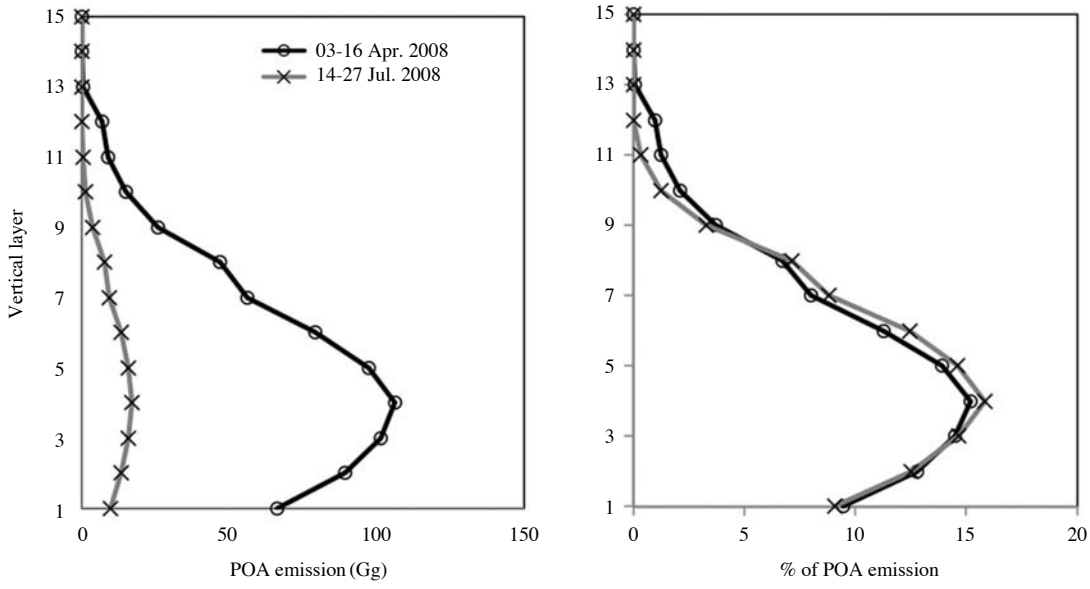

Fig. 9. Vertical distribution of POA emission from biomass burning during modeling period.

system using factors. Using temporal profiles from the SMOKE modeling system, temporally resolved emissions (i.e., at 1-h time intervals) could be generated from the daily inventories. The chemical speciation process converts inventory pollutants such as CO, NO_x, VOC, SO_2, and $PM_{2.5}$ into model species using air-quality models. The spatial processing generally combines the grid specification for the air-quality model domain with source locations from the inventory file (Houyoux *et al.*, 2007).

Fig. 8 shows model-ready primary-organic-aerosol (POA) emissions from anthropogenic sources (Woo *et al.*, 2012) and integrated sources of anthropogenic and biomass-burning sources (in this study) during the modeling period. Spatially, Siberia shows higher POA emissions from open biomass burning than other regions, and the largest emission occurred during April, as compared to July. In contrast, emissions from anthropogenic sources in both April and July show similar levels despite their temporal patterns. In the case of July, the northern part of Siberia was more affected by fires compared to April.

The fire-plume-rise algorithm included in the SMOKE modeling system can transform each fire event into three-dimensional hourly emissions. Vertically distributed total POA emissions from open biomass burning during the entire modeling period were aggregated, as shown in Fig. 9. From this study, it was found that effectively no emissions were released beyond the 14th and 12th vertical layers of the model (approximately 6,000 m and 4,000 m above ground level (AGL)) in April and July, respectively. Most of the emissions were located under layer 7, which broadly corresponds to the altitude ranging from 0 to 1,000 m AGL.

Table 2. Comparison of the biomass-burning emissions calculated in our study with other published estimates in our domain (April 2008).[a]

Pollutant and study	East Asia	Southeast Asia	South Asia	Siberia
CO				
This work	1.42	0.45	1.43	24.83
GFEDv3	1.30	2.02	1.09	16.34
Streets *et al.* (2003)[b]	4.95	4.25	0.75	
$PM_{2.5}$[c]				
This work	0.16	0.05	0.16	2.53
GFEDv3	0.13	0.18	0.10	1.84

[a]Units are Gg/month. [b]This study estimated "typical" (non-year-specific) biomass burning emissions. [c]Not included in Streets *et al.* (2003) reference.

4. EMISSION VALIDATION

4. 1 Comparison of Estimated Emissions from the BlueSky Framework and from the Previous Studies

The biomass-burning CO emission estimates during April 2008 using the BlueSky framework were compared with those of two previous studies. The first is the study of Streets *et al.* (2003), who established a set of "typical" (i.e., non-year-specific) emissions inventories from open biomass burning for the Asian region during the mid-1990s to support the ACE-Asia and

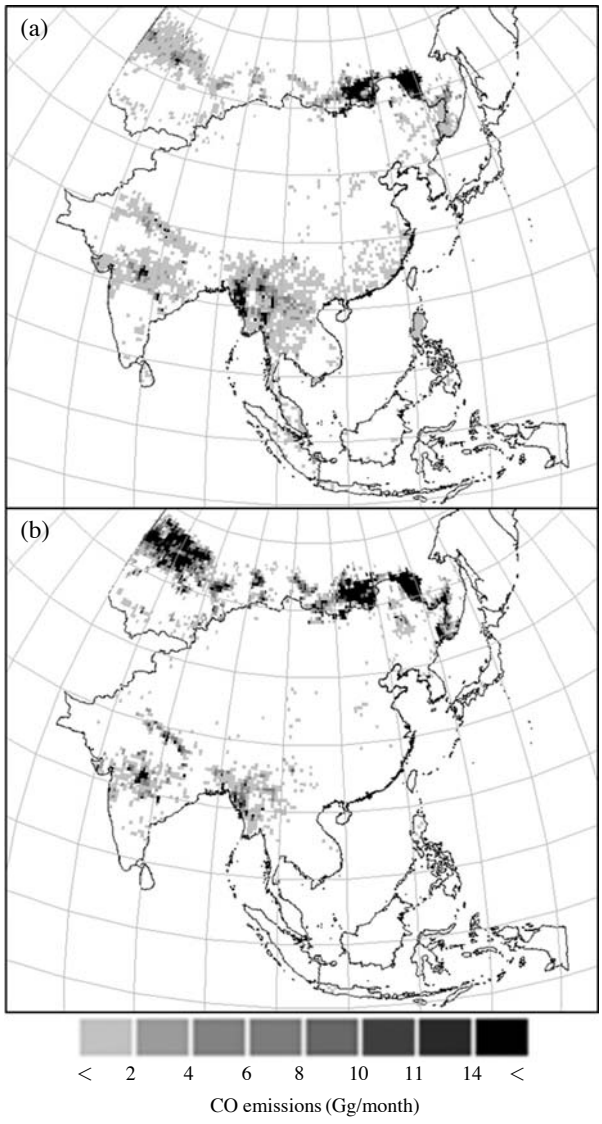

Fig. 10. Distribution of CO emissions estimated from (a) GFEDv3 and (b) this study during April 2008.

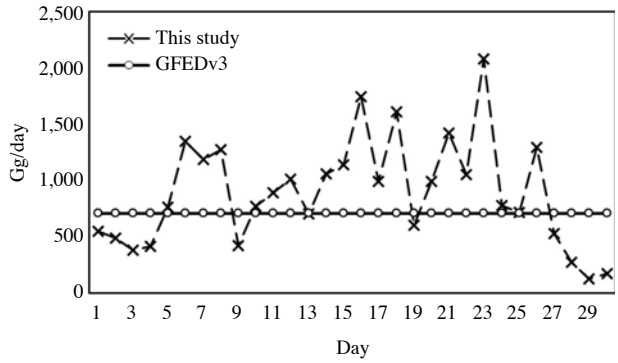

Fig. 11. Comparison of daily variations of CO emissions between this study and time-resolved GFEDv3 during April 2008.

TRACE-P campaigns. The other is the Global Fire Emissions Database Version 3 (GFEDv3) inventory (Giglio *et al.*, 2010; van der Werf *et al.*, 2010). As shown in Table 2, our results show good to fair agreement with GFEDv3, which is recently updated using the improved burned area data sets, for most regions except Southeast Asia, with differences ranging from 9.7% (in East Asia) to 52% (in Siberia). This may be because they were based on similar remote-sensing products such as MODIS. The CO emissions estimate for Southeast Asia from the BlueSky framework appears to be about 78% lower than that from GFEDv3, because of limited satellite detection due to cloud interference (Fig. 10). In contrast, the estimates by Streets *et al.* (2003) were 2.2-3 times those of GFEDv3 or of this study across all of Asia. This difference was mainly caused by the fire information used for estimating biomass-burning emissions. The emissions by Streets *et al.* (2003) were estimated using ground-based data from the literature from the 1950s to the 1990s, which are rather old considering the rapid changes in population growth and land use throughout Asia. Despite the limitations on satellite observations, such as cloud contamination, biomass-burning emissions derived from remote-sensing data (e.g., satellite measurements) can provide a series of quantitative observations that have better spatial and temporal distributions than a "typical" bottom-up emissions inventory. Fig. 11 shows the comparison of daily CO emissions between our results and those of time-resolved GFEDv3 during April 2008. Daily emissions from each fire event were used in this study, whereas monthly emissions were applied to the GFED inventory. A monthly variation in the biomass-burning estimation would be good enough for global-scale modeling but may be too coarse for regional-scale emissions and transport.

4.2 Analysis of Discrepancies with Input Parameters

4.2.1 Comparison of Satellite Data Products

We compared MODIS burned-area products with MODIS active-fire products during our test case (April and July, 2008) to check the consistency between two different fire retrieval algorithms for the same time and location. We assumed that each active fire had a burned area of 1 km^2, which is equal to the detection resolution.

Fig. 12 shows a comparison between daily burned-area estimates in our domain using the MODIS active-

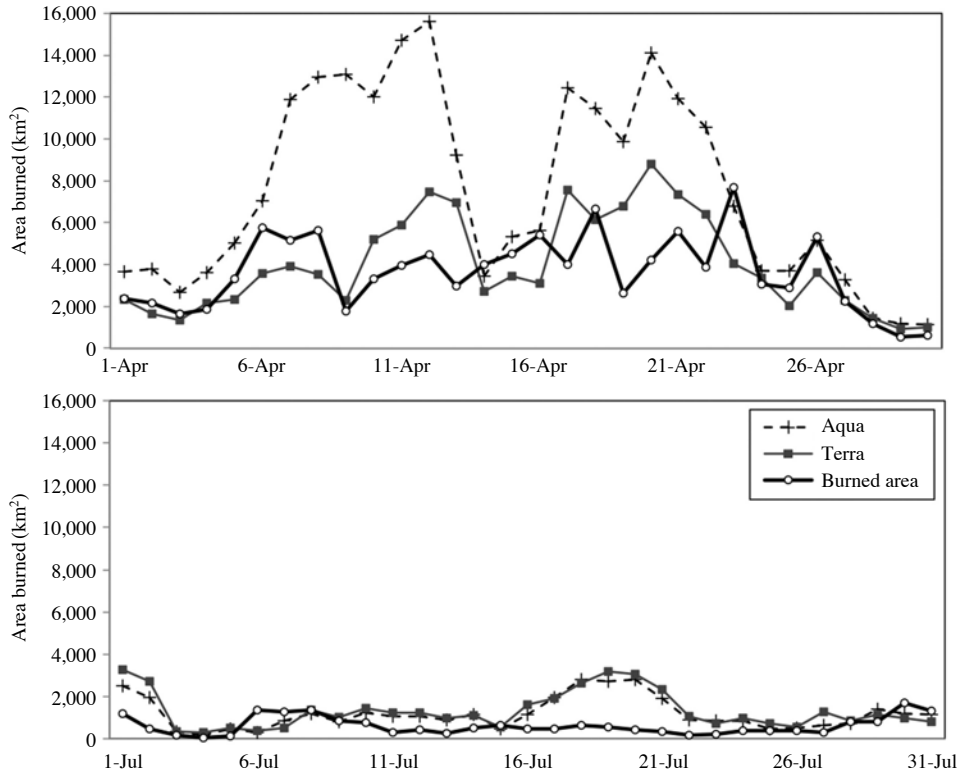

Fig. 12. Comparison between MODIS fire products during study periods (upper panel: April 2008; lower panel: July 2008).

fire product from both Aqua and Terra satellites, and MODIS burned-area products. In theory, they should be identical. In our test cases, however, burned-area products showed a much smaller total area burned than the active-fire products. As mentioned in Section 2.2, the two MODIS products employ different algorithms for estimating fire information, which could influence the spatiotemporal fire characteristics as well as quantitative results. The MODIS burned-area algorithm detects the approximate date of burning at a 500-m resolution by locating the occurrence of rapid changes in the daily surface-reflectance time-series data, whereas the MODIS active-fire product detects fires in 1-km pixels that are burning at the time of overpass under relatively cloud-free conditions (Giglio *et al*., 2003). Global evaluation by comparison of the two MODIS products was described in Roy *et al*. (2008). We also compared active-fire products from the same MODIS sensors in Aqua and Terra to check consistency between the two datasets with the same retrieval algorithm. Despite using the same retrieval algorithm, the MODIS sensors in Terra and Aqua produced very different active fires.

Fig. 13 shows a comparison of the active-fire products from the MODIS sensors onboard Terra and Aqua for April and July 2008 periods. The correlation between the two active-fire products for Siberia and Kazakhstan was relatively high ($0.85 < R^2 < 0.96$) compared to those for other regions. East Asia, Southeast Asia, and South Asia, however, exhibited poor correlation between the two satellite instruments, especially in July ($R^2 < 0.29$). The East Asia region displayed much lower correlation in July than in April, which could be caused by monsoon and cloud contamination effects. Giglio *et al*. (2006) presented a similar case in which eastern China was classified into a lower cross-correlation region (correlation coefficient of 0.62) in the Terra /Aqua time series comparisons during July 2002 to October 2005 (e.g., for Southeast Russia, 0.99; for Southern Africa, 0.98; for Northern Australia, 0.96).

4. 2. 2 Burned Area by Vegetation Type

The emission estimates for April and July showed significant differences by region, as a result of the type of vegetation burned as well as the area burned. The upper and lower panels of Fig. 14 show the area burned by vegetation for April and July, respectively. The land cover classes representing smaller plants, such as savannas, grasslands, and croplands, accounted for most burning over the SASIA (South Asia) and East Asia regions. In Siberia, however, the main vegetation types burned differed between April and July. In April,

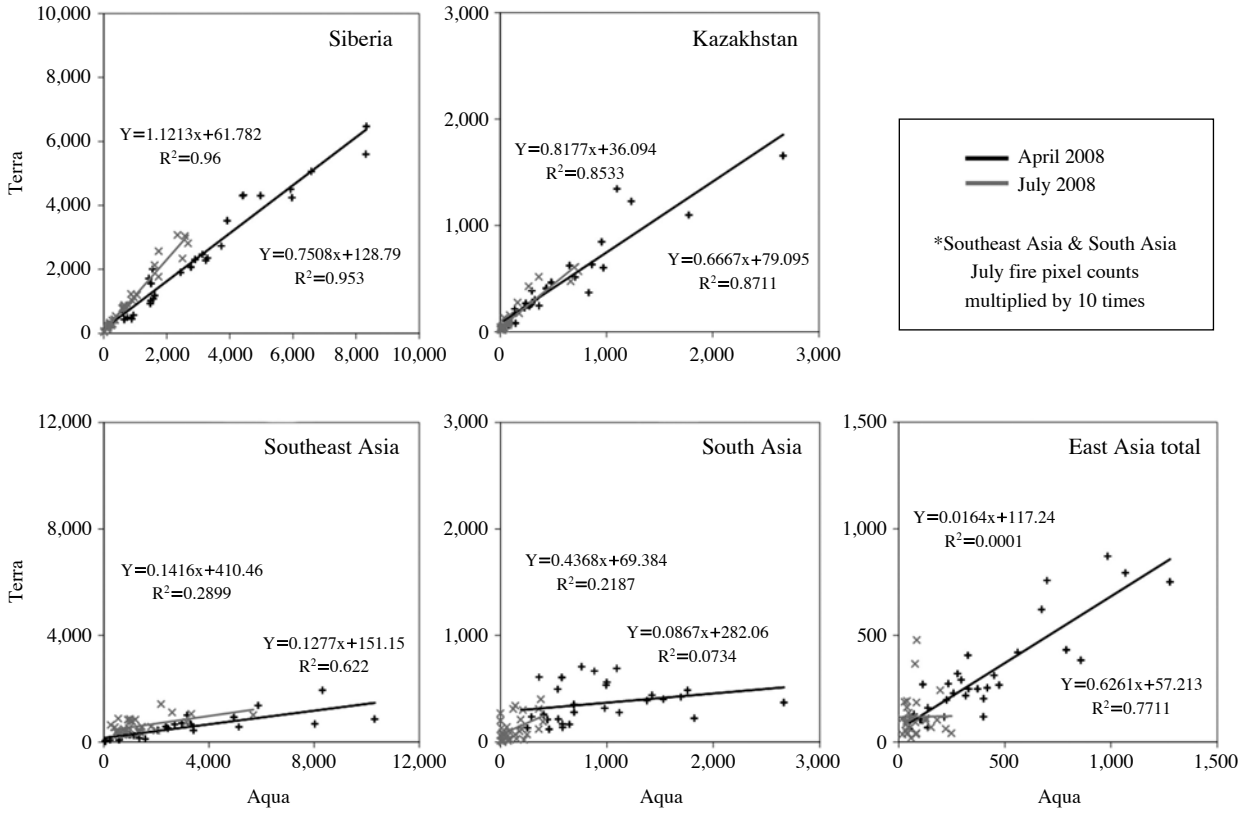

Fig. 13. Correlation between Terra and Aqua daily fire pixels for each region during April and July 2008.

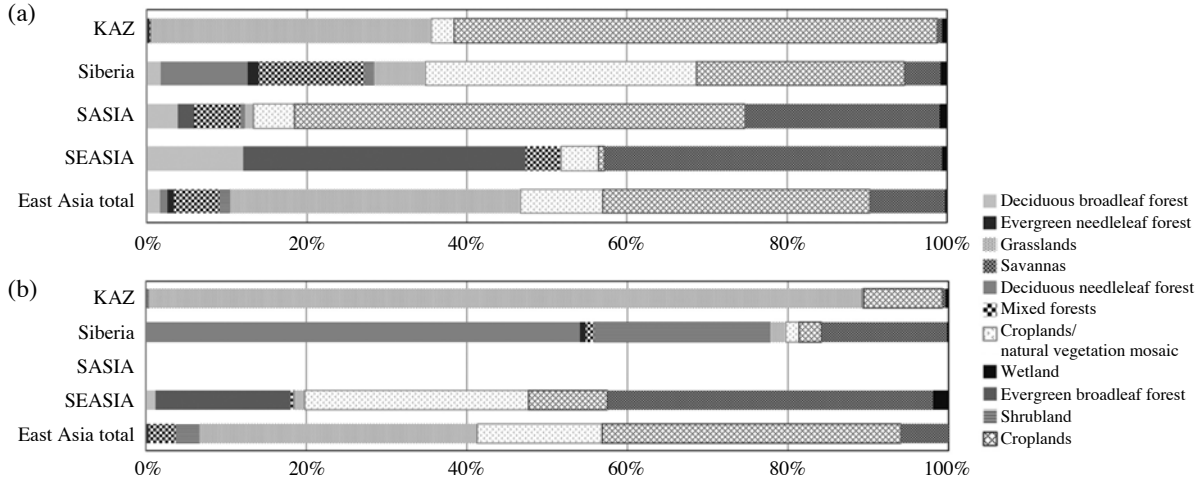

Fig. 14. The portion of burned areas for each vegetation type in (a) April and (b) July 2008.

cropland was the main class of vegetation burned, contributing approximately 65% of the total burned area, but in July, forest was the prevalent class. In Kazakhstan, grassland and cropland were the major classes of vegetation burned and also showed a clear difference by season.

5. SUMMARY AND CONCLUSIONS

A biomass-burning emissions modeling system for Asia using the BlueSky Framework, developed by US Forest Service (USFS) and the US Environmental Protection Agency (EPA), was developed to support air-

quality modeling and analysis using the SMOKE modeling system.

To build a successful emissions system for Asia, the processing of fire information and the development of a fuel map associated with fuel classification based on regional characteristics as well as the modification of system codes were required. Hence, we used the MODIS burned-area product (MCD45A1) to estimate the amount of emissions from open biomass burning in the Asian region for April and July 2008. We also developed a new Asian fuel map with 7 FCCS classes based on the MODIS 2008 land cover product (MCD 12Q1, Land cover type 1-IGBP) to estimate fuel loading over Asia. Moreover, we combined the BlueSky framework and the SMOKE modeling system to improve air-quality modeling by using more temporally and spatially accurate biomass-burning emissions.

In this study, biomass-burning emissions of CO, $PM_{2.5}$, and NMHC were derived using the BlueSky Framework for Asia during April and July 2008. Quantitative evaluation of our results was conducted by comparing them with the emissions estimates of GFEDv3, which is an inventory widely used among experts, from month to month. Our results showed good agreement with the estimates of GFEDv3 for most regions except for Southeast Asia. This is because they are both based on the same remote-sensing products such as MODIS. Furthermore, by comparing MODIS burned-area products with MODIS active-fire products during our test cases, it was found that the fire emission characteristics were influenced by the different algorithms for estimating fire information, as well as by monsoon and cloud contamination effects. Finally, we found that the emission estimates for April and July showed significant differences by region due to the type of vegetation burned and area burned.

By integrating the BlueSky framework into the SMOKE modeling system, daily biomass-burning emission inventories were transformed into spatiotemporally resolved and chemically speciated three-dimensional model-ready emissions, which could be useful for comprehensive regional-scale atmospheric chemistry models. We hope that the results of this study can provide better air-quality model input data and further help to understand the impact of air-pollutant emissions on Asian air quality.

ACKNOWLEDGEMENT

This work was funded by the Korea Meteorological Administration Research and Development Program under Grant CATER 2012-6123.

REFERENCES

Anderson, K.G., Sandberg, V.D., Norheim, A.R. (2004) Fire Emission Production Simulator (FEPS) User's Guide. U.S. Forest Service.

Belward, A.S., Estes, J.E., Kline, K.D. (1999) The IGBP-DIS Global 1-km Land-Cover Data Set DISCover: A Project Overview. Photogrammetric Engineering and Remote Sensing 65, 1013-1020.

Burgan, R.E., Klaver, R.W., Klaver, J.M. (1998) Fuel Models and Fire Potential from Satellite and Surface Observations. International Journal of Wildland Fire 8(3), 159-170.

Giglio, L., Descloitres, J., Justice, C.O., Kaufman, Y. (2003) An enhanced contextual fire detection algorithm for MODIS. Remote Sensing of Environment 87, 273-282.

Giglio, L., Csiszar, I., Justice, C. O. (2006) Global distribution and seasonality of active fires as observed with the Terra and Aqua Moderate Resolution Imaging Spectroradiometer (MODIS) sensors. Journal of Geophysical Research 111, G02016, doi:10.1029/2005JG000142.

Giglio, L., Randerson, J.T., van der Werf, G.R., Kasibhatla, P.S., Collatz, G.J., Morton, D.C., DeFries, R.S. (2010) Assessing variability and long-term trends in burned area by merging multiple satellite fire products. Biogeosciences 7, 1171-1186.

Hardy, C., Menakis, J.P., Garner, J.L. (1998) FMI/WESTAR emissions inventory and spatial data for the western United States, USDA Forest Service, Rocky Mountain Research Station, Fire Sciences Laboratory, Missoula, MT.

Houyoux, M.R., Vukovich, J.M., Brandmeyer, J. (2007) SMOKE User Manual, version 2.3., MCNC Environmental Programs, Research Triangle Park, NC, USA.

Jeong, J.I., Park, R.J., Youn, D. (2008) Effects of Siberian forest fires on air quality in East Asia during May 2003 and its climate implication. Atmospheric Environment 42, 8910-8922.

Kuenzli, N., Avol, E., Wu, J., Gauderman, W.J., Rappaport, E., Millstein, J., Bennion, J., McConnell, R., Gilliland, F.D., Berhane, K. (2006) Health effects of the 2003 southern California wildfire on children. American Journal of Respiratory and Critical Care Medicine 174, 1221-1228.

McKenzie, D., Kopper, K.E., Bayard, A.C. (2004) A rule-based fuzzy classification for landscape modeling of fuel succession. Proceedings of the 2003 Sydney Fire Conference.

Michel, C., Liousse, C., gregoire, J.M., Tansey, K., Carmichael, G.R., Woo J.-H. (2005) Biomass burning emission inventory from burnt area data given by the SPOT-VEGETATION system in the frame of TRACE-P and ACE-Asia campaigns. Journal of Geophysical Research 110, D09304, doi:10.1029/2004JD005461.

MOE (Ministry Of Environment) (2009) Development of

high-resolution meteorological-atmospheric chemistry modeling system for support urban-scale PM forecast.

Ottmar, R.D., Burns, M.F., Hall, J.N., Hanson, A.D. (1993) CONSUME users guide. USDA Forest Service General Technical Report PNWGTR-304. Pacific Northwest Research Station, Portland, OR.

Pouliot, G., Pierce, T., Benjey, W. (2005) Wildfire Emission Modeling: Integrating BlueSky and SMOKE. 14th International Emission Inventory Conference. "Transforming Emission Inventories Meeting Future Challenges Today".

Pryden, A.D. (2008) Getting started with the BlueSky Framework version 3.0. Sonoma Technology, Inc.

Roy, D.P., Lewis, P.E., Justice, C.O. (2002). Burned area mapping using multi-temporal moderate spatial resolution data-a bi-directional reflectance model-based expectation approach. Remote Sensing of Environment 83, 263-286.

Roy, D.P., Jin, Y., Lewis, P.E., Justice, C.O. (2005). Prototyping a global algorithm for systematic fire affected area mapping using MODIS time series data. Remote Sensing of Environment 97, 137-162.

Roy, D.P., Boschetti, L., Justice, C.O., Ju, J. (2008) The Collection 5 MODIS Burned Area Product - Global Evaluation by Comparison with the MODIS Active Fire Product. Remote Sensing of Environment 112, 3690-3707.

Sandberg, D.V., Peterson, J.L. (1984) A source strength model for prescribed fires in coniferous logging slash. In: Proceedings, 21st annual meeting of the Air Pollution Control Association, Pacific Northwest International Section, 1984 November 12-14, Portland, OR. Pittsburgh, PA: Air Pollution Control Association.

Sandberg, D., Ottmar, R., Cushon, G. (2001) Characterizing fuels in the 21st century. International Journal of Wildland Fire 10, 381-387.

Scepan, J. (1999) Thematic Validation of High-Resolution Global Land-Cover Data Sets. Photogrammetric Engineering and Remote Sensing 65, 1051-1060.

Streets, D.G., Yarber, K.F., Woo, J.-H., Carmichael, G.R. (2003) Biomass burning in Asia: Annual and seasonal estimates and atmospheric emissions. Global Biogeochemical Cycles 17(4), 1099, doi:10.1029/2003GB002040.

Tanimoto, H., Kajii, Y., Hirokawa, J., Akimoto, H., Minko, N.P. (2000) The atmospheric impact of boreal forest fires in far eastern Siberia on the seasonal variation of carbon monoxide: Observations at Rishiri, A northern remote island in Japan. Geophysical Research Letters 27(24), 4073-4076.

van der Werf, G.R., Randerson, J.T., Giglio, L., Collatz, G.J., Kasibhatla, P.S., Arellano, A.F. (2006) Interannual variability in global biomass burning emissions from 1997 to 2004. Atmospheric Chemistry and Physics 6, 3423-3441.

van der Werf, G.R., Randerson, J.T., Giglio, L., Collatz, G.J., Mu, M., Kasibhatla, P.S., Morton, D.C. (2010) Global fire emissions and the contribution of deforestation, savanna, forest, agricultural, and peat fires (1997-2009). Atmospheric Chemistry and Physics 10, 11707-11735.

Woo, J.-H., Streets, D.G., Carmichael, G.R., Tang, Y., Yoo, B., Lee, W., Thongboonchoo, N., Pinnock, S., Kurata, G., Uno, I., Fu, Q., Vay, S., Sachse, G.W., Blake, D.R., Fried, A., Thornton, D.C. (2003) The Contribution of Biomass and Biofuel Emissions to Trace Gas Distributions in Asia during the TRACE-P Experiment. Journal of Geophysical Research 108(D21), 8812, doi:10.1029/2002JD003200.

Woo, J.-H., Choi, K.-C., Kim, H.K., Baek, B.H., Jang, M., Eum, J.-H., Song, C.H., Ma, Y.-I., Sunwoo, Y., Chang, L.-S. and Yoo, S.H. (2012) Development of an anthropogenic emissions processing system for Asia using SMOKE, Atmospheric Environment, 58, 5-13.

Yevich, R., Logan, J.A. (2003) An assessment of biofuel use and burning of agricultural waste in the developing world. Global Biogeochemical Cycles 17(4), 1095.

(Received 30 August 2011, revised 26 November 2012, accepted 10 January 2013)